Supporting information

Lithiophilic Sb Surface Modified Cu Nanowires Grown on Cu Foam: A Synergy of 1D@3D Hierarchical Structure toward Stable Lithium Metal Anodes

Xuelian Fu[1#], Chaoqun Shang[2#]*, Guofu Zhou[1], Xin Wang[1]*

[1]Guangdong Provincial Key Laboratory of Optical Information Materials and Technology, South China Academy of Advanced Optoelectronics, South China Normal University, Guangzhou 510006, China

[2]Hubei Key Laboratory of Plasma Chemistry and Advanced Materials, School of Materials Science and Engineering, Wuhan Institute of Technology, Wuhan 430205, China

[#]These authors contributed equally.

Corresponding Author

*Chaoqun Shang, E-mail: chaoqun.shang@foxmail.com

*Xin Wang, E-mail: wangxin@scnu.edu.cn

Experimental section

Preparation of 1D@3D-Cu/Sb

The commercial Cu foam (0.5 mm in thickness) was first cut into wafers with a diameter of 12 mm and washed several times in an ultrasonic bath with absolute ethanol, diluted HCl solution and deionized water to remove surface contaminations. Then, the pre-treated Cu foam slices were immersed into 10 mL aqueous solution containing 2.5 M NaOH and 0.13 M $(NH_4)_2S_2O_8$ at room temperature for 2 min. After that, the light-blue Cu foam discs with $Cu(OH)_2$ nanowires (1D@3D-$Cu(OH)_2$) was cleaned ultrasonically 5 times in deionized water until the pH reached 7 to ensure that a tight connection between the nanowires and the Cu foam and then dried in oven. The prepared 1D@3D-$Cu(OH)_2$ was heated in tube furnace at 200 ℃ under 5% (v/v) H_2/Ar for 80 min to obtain Cu foam with Cu nanowires (1D@3D-Cu). The 1D@3D-Cu was then collected and immediately soaked into an ethanol solution of 5 mL of $SbCl_3$ (0.02 M) for 5 minutes. Finally, the prepared sample was washed ultrasonically several times in absolute ethanol bath and dried in a vacuum oven at 40 ℃ for 10 h.

Materials characterization

The morphological characteristics of as-prepared materials were observed using a field-emission scanning electron microscope (FESEM, TESCAN MIRA3) with an energy dispersive X-ray spectrometer (EDS, Oxford X-MaxN50) system. Before the SEM test, the Li-deposited samples were disassembled from the cells in an argon-filled glove box, and were gently washed with 1,2-dimethoxyethane (DME) to remove

residual electrolyte. Transmission electron microscopy (TEM) and scanning transmission electron microscopy (STEM) were measured by the JEOL JEM 2100F apparatus with EDS system. The changes on the surface chemistry of materials were checked using X-ray photoelectron spectroscopic (XPS, Thermo Scientific NEXSA) with Al-Kα source (hv = 1486.6 eV). The nitrogen absorption-desorption isotherms were measured at 77 K on a Gold APP Istruments V-Sorb X800 and the specific surface area was calculated by the Brunauer-Emmett-Teller (BET) method. Chemical compositions were determined with inductively coupled plasma (ICP) analysis performed on an Aglient 5110 ICP spectrometer.

Electrochemical measurements

Type-CR2032 coin cells were assembled with polypropylene (PP) (Celgard 2500) separator for all electrochemical measurements in an argon-filled glove box ($H_2O \leq 0.1$ ppm, $O_2 \leq 0.1$ ppm). To standardize the test, 80 μL electrolyte (1.0 M lithium bis(trifluoromethanesulfonyl)imide (LiTFSI) in a mixture solvent of 1,3-dioxolane (DOL) and DME (1:1 by volume) with 1 % lithium nitrite ($LiNO_3$) as an additive) was added into each coin cell. The electrochemical measurements and plating/stripping of Li were performed on a battery test system (CT-4008, NEWARE).

Cyclic voltammogram (CV) measurements were conducted to determine the double-layer capacitance (C_{dl}) of 3D-Cu, 1D@3D-Cu and 1D@3D-Cu/Sb, which were expected to be linearly proportional to electrochemically active surface areas. The half cells were assembled using 3D-Cu, 1D@3D-Cu and 1D@3D-Cu/Sb as the working electrodes and Li foil as the reference and counter electrodes. The assembled batteries

were first pre-cycled between 0.01 and 0.5 V at the current of 0.05 mA for 5 cycles to activate the cells and stabilize interface between electrolyte and electrodes. To evaluate the CEs of half cells, Li was deposited onto the current collector at different current densities and then stripping the Li metal until the charge potential up to 0.5 V at the same current density for each cycle. During the symmetric cells tests and the full cells tests, 4 mAh cm^{-2} of Li were pre-deposited on 3D-Cu, 1D@3D-Cu and 1D@3D-Cu/Sb at a current density of 0.5 mA cm^{-2} to get 3D-Cu-Li, 1D@3D-Cu-Li and 1D@3D-Cu/Sb-Li anodes. The Li||current collector-based composite Li electrode (Li||current collector-Li) cells were tested with the stripping/plating of 1 mAh cm^{-2} of Li at 1 mA cm^{-2}, 2 mA cm^{-2}, 3 mA cm^{-2}, and 5 mA cm^{-2}, respectively. Electrochemical impedance spectroscopy (EIS) was measured with an electrochemical workstation (Bio-logic VMP3) in a frequency range from 10^5 Hz to 10^{-1} Hz with an amplitude of 5 mV. The CV was tested on the electrochemical workstation at a scan rate of 0.2 mV s^{-1} in the scan range from 0 to 2.4 V.

The full cell composes of 3D-Cu-Li, 1D@3D-Cu-Li and 1D@3D-Cu/Sb-Li anodes and LFP cathode. LFP cathode was prepared by mixing the active material (LFP), conductive agent (super-P) and binder (PVDF) with a weight ratio of 8:1:1 in NMP. Then, the as-prepared uniform slurry was casted on Al foil and dried at 100 ^oC under vacuum for 10 h and then punched into 12 mm disks for assembly of battery. The LFP mass loading on cathode was about 2 mg cm^{-2}. The as-assembled full cells were tested between 2.5 V and 4.0 V at different rates.

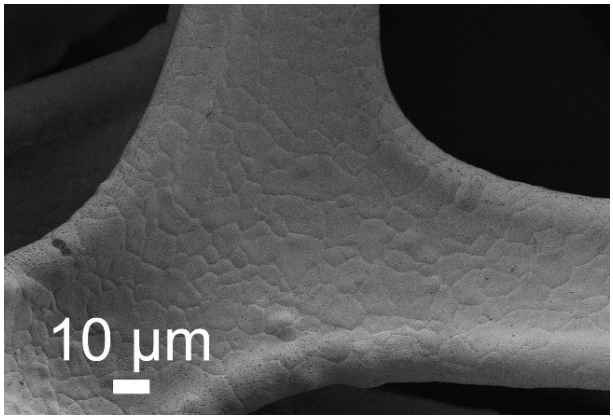

Figure S1. SEM image of 3D-Cu.

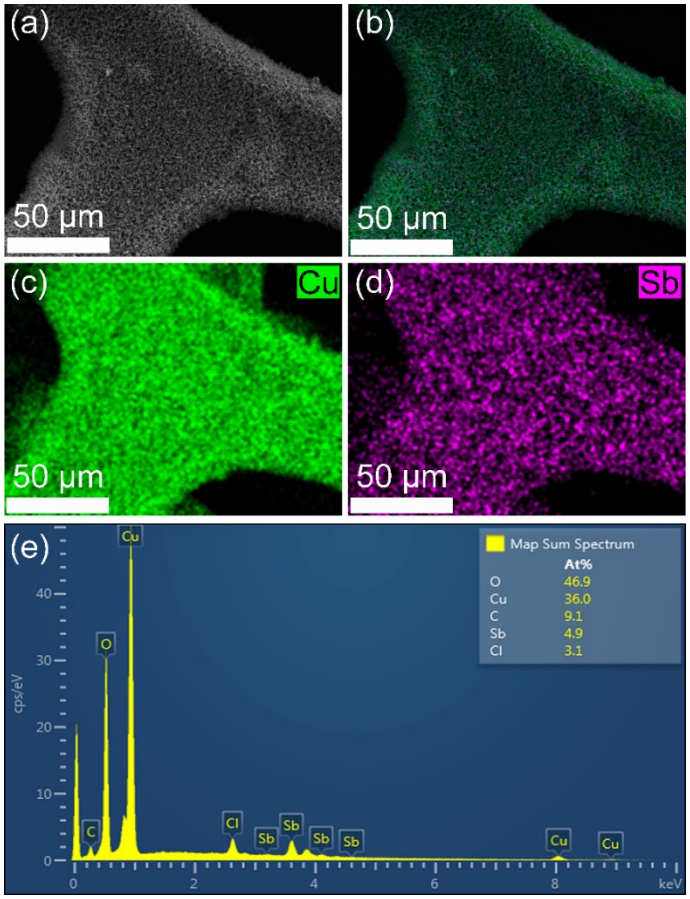

Figure S2. (a, b) SEM images of 1D@3D-Cu/Sb. EDS elemental mapping images of (c) Cu and (d) Sb of the 1D@3D-Cu/Sb. (e) EDS spectra of the 1D@3D-Cu/Sb.

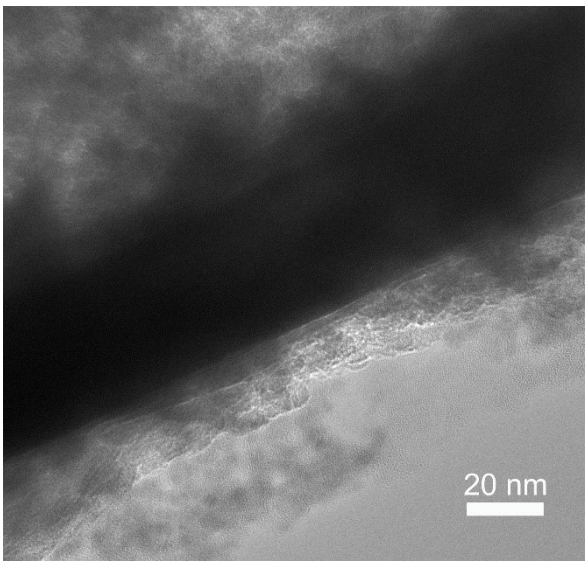

Figure S3. The TEM image of 1D@3D-Cu/Sb.

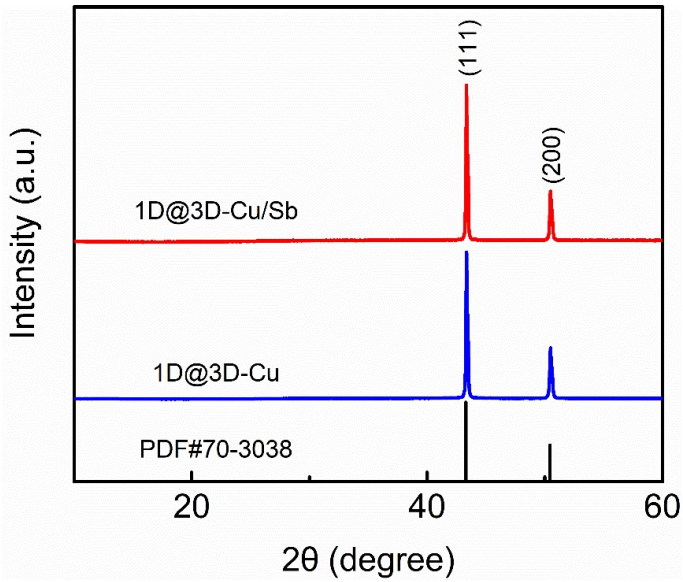

Figure S4. XRD patterns of 1D@3D-Cu/Sb and 1D@3D-Cu.

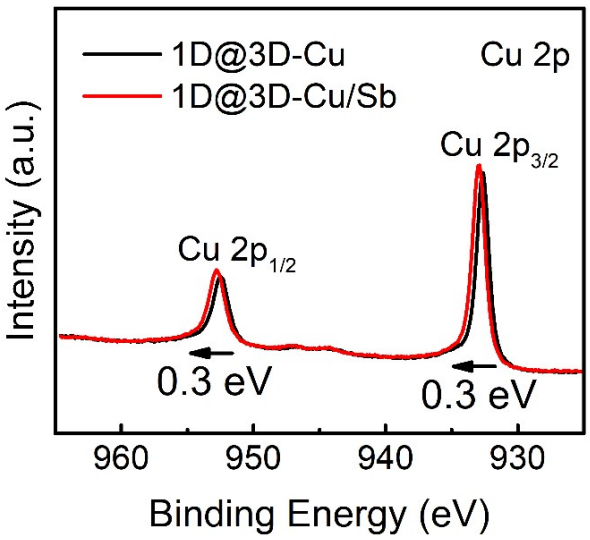

Figure S5. The raw data of high-resolution Cu 2p XPS spectrum of 1D@3D-Cu and 1D@3D-Cu/Sb.

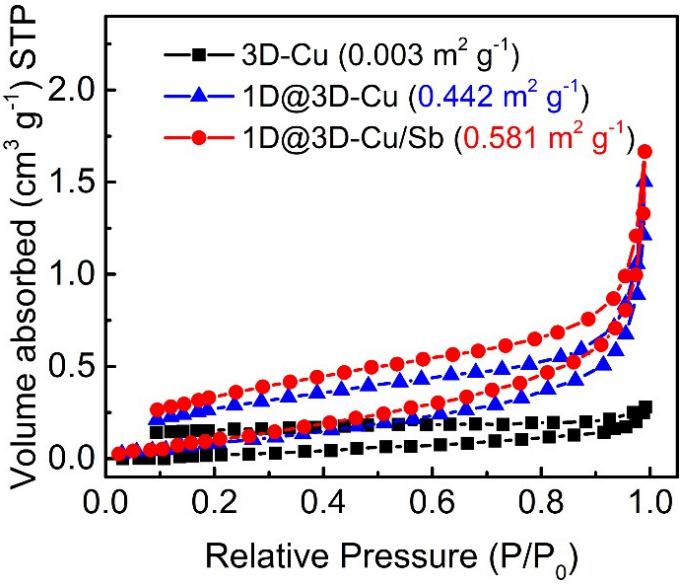

Figure S6. The nitrogen adsorption/desorption isotherms of the 3D-Cu, 1D@3D-Cu and 1D@3D-Cu/Sb samples.

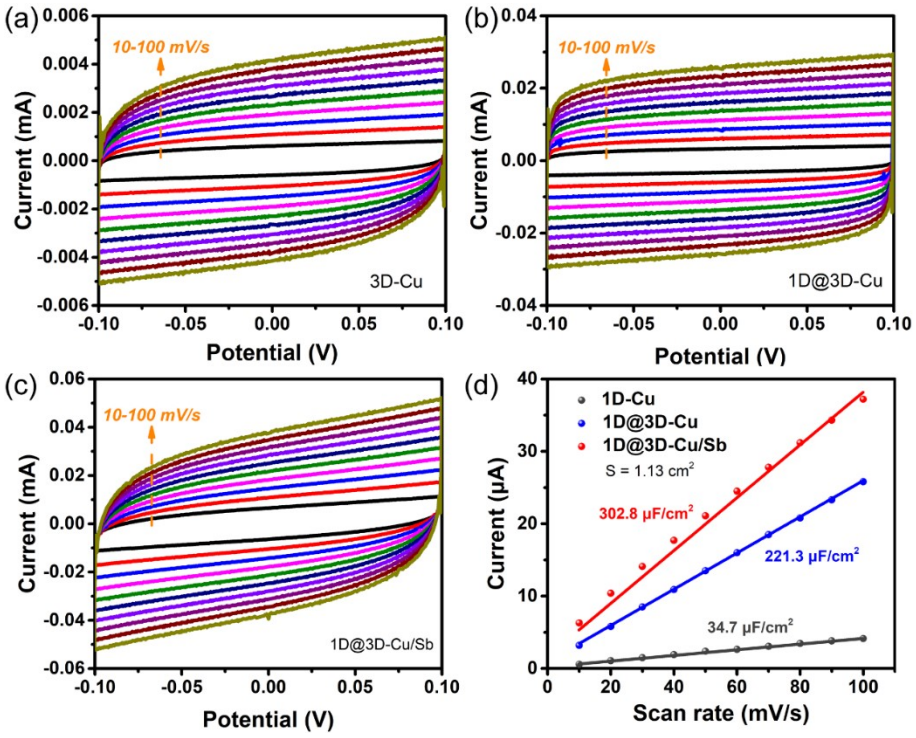

Figure S7. Cyclic voltammograms of (a) 3D-Cu, (b) 1D@3D-Cu and (c) 1D@3D-Cu/Sb. (d) Difference in current ($\Delta I = I_a - I_c$) at 0 V plotted versus scan rate fitted to a linear regression for the calculation of double-layer capacitance (C_{dl}) of 3D-Cu, 1D@3D-Cu and 1D@3D-Cu/Sb.

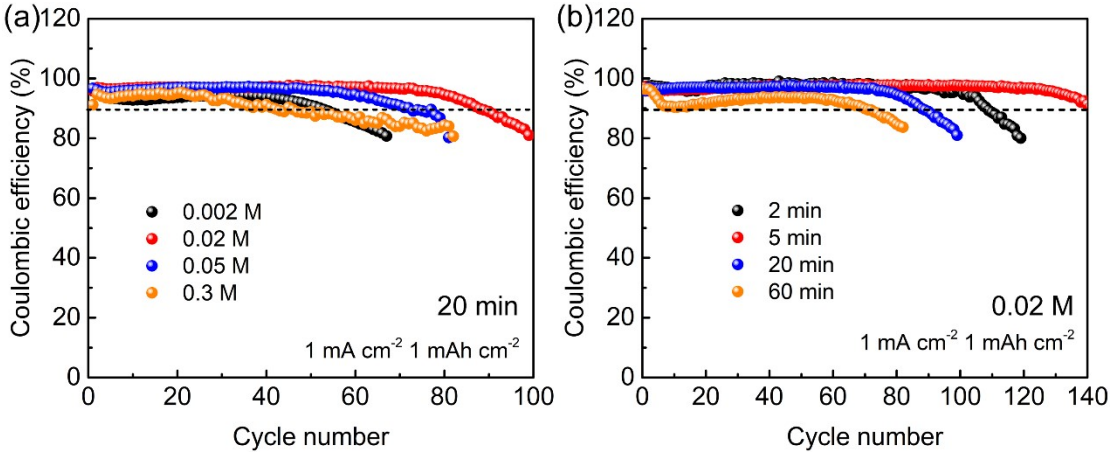

Figure S8. Coulombic efficiencies of Li plating/stripping on the 1D@3D-Cu/Sb with current density of 1 mA cm^{-2} and Li deposition of 1 mAh cm^{-2} under (a) different concentration of $SbCl_3$ solution and (b) different duration of replacement reaction.

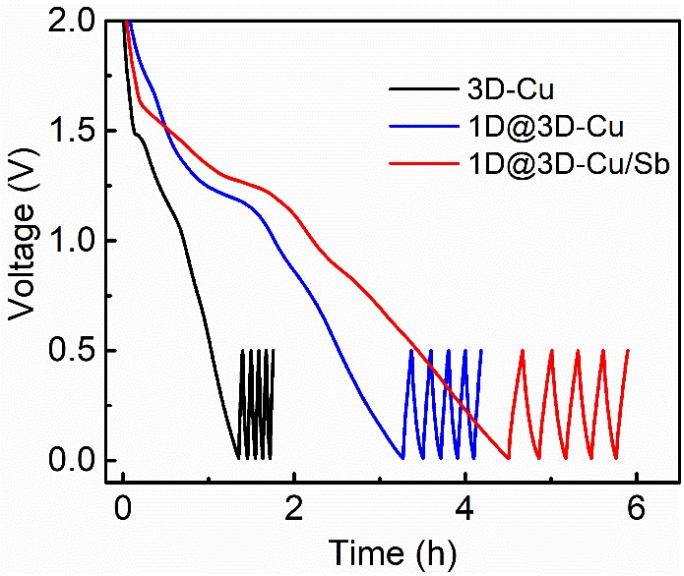

Figure S9. Voltage-time profiles during initial activation process. The cells were first cycled between 0.01-0.5 V (vs. Li^+/Li) at 50 μA for five cycles to form a SEI layer.

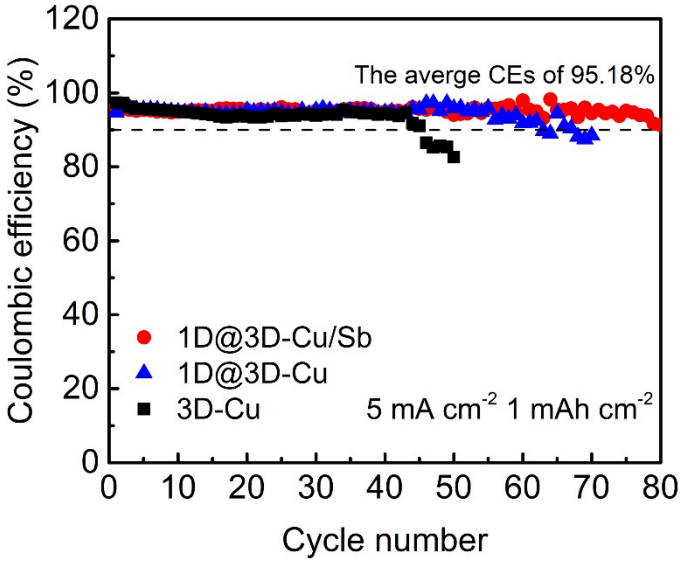

Figure S10. Coulombic efficiencies of Li plating/stripping on different current collectors with current density of 5 mA cm^{-2} for a total Li deposition of 1 mAh cm^{-2}.

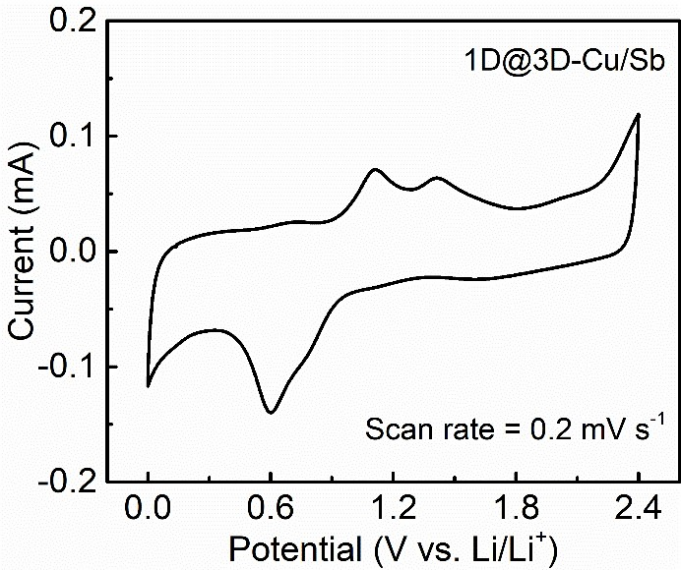

Figure S11. CV curve of 1D@3D-Cu/Sb at 0.2 mV s^{-1}.

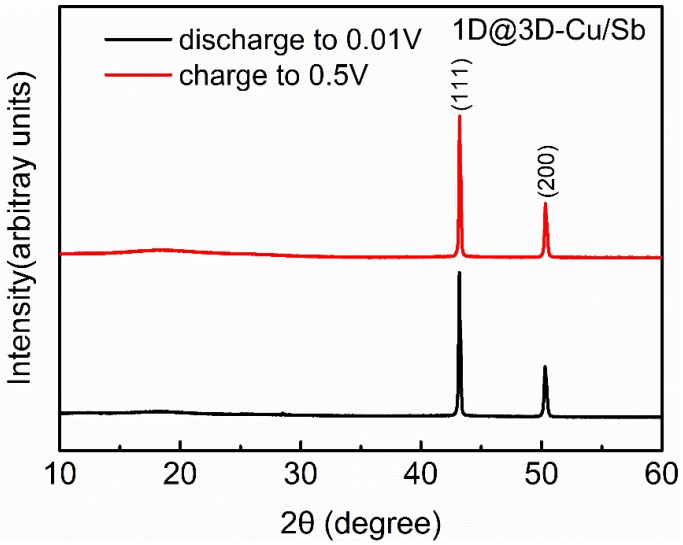

Figure S12. XRD patterns of the 1D@3D-Cu/Sb discharge to 0.01 V and charge to 0.5 V.

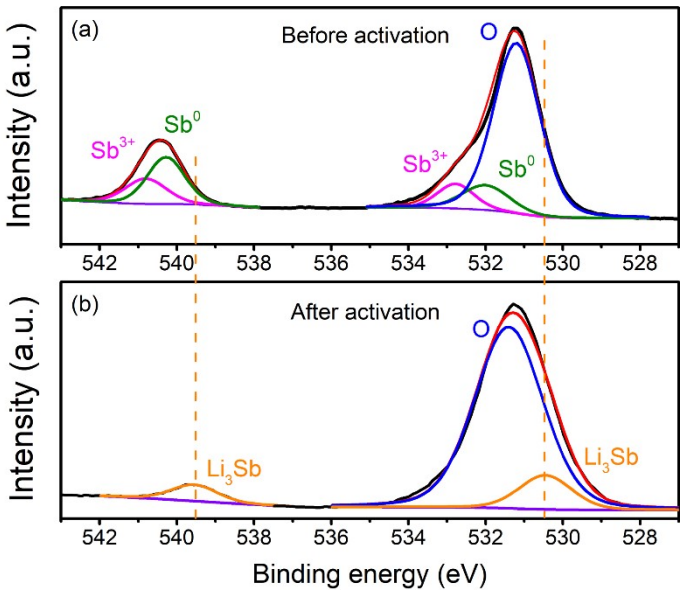

Figure S13. High-resolution Sb 3d XPS spectrum of 1D@3D-Cu/Sb (a) before and (b) after activation process.

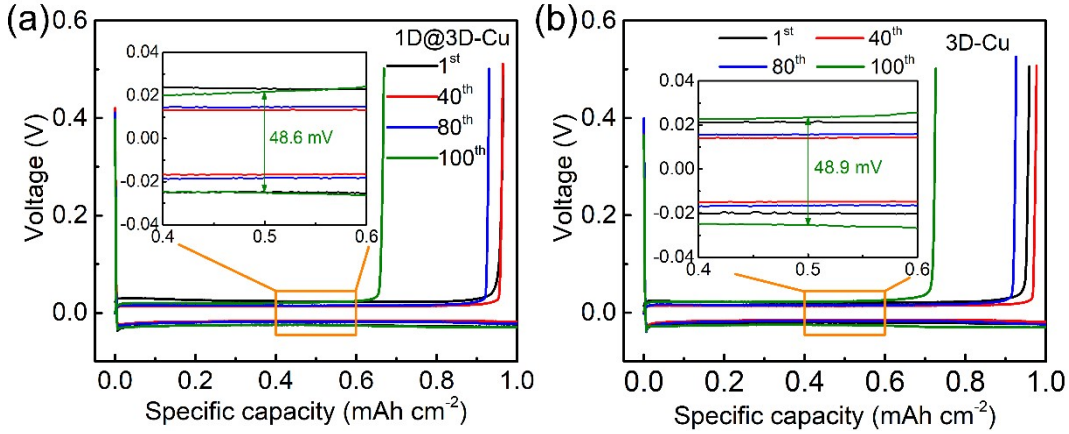

Figure S14. The Li deposition/stripping profiles on (a) 1D@3D-Cu and (b) 3D-Cu (1 mA cm^{-2}, 1 mAh cm^{-2}).

Table S1. Comparison of the Coulombic efficiencies between the 1D@3D-Cu/Sb current collectors and other lithiophilic Cu-based current collectors.

Current collector	**Electrolyte & dosage**	**Current density [mA cm^{-2}]**	**Areal capacity [mAh cm^{-2}]**	**Cycle number**	**CE [%]**	**Ref.**
Cu fiber @Cu foam	1 M LiTFSI in 1:1 (v/v) DOL/DME with 2% $LiNO_3$ (-)	1	1	200	98	1
Cu_2S NWs @Cu foam	1 M LiTFSI in 1:1 (v/v) DOL/DME with 1% $LiNO_3$ (40 μL)	1	1	500	99.2	2
		2	2	300	98.5	
		4	4	100	98	
Cu_2S NWs @Cu foam	1 M LiTFSI in 1:1 (v/v) DOL/DME with 1% $LiNO_3$ (50 μL)	1	1	150	95.5	3
		2	1	150	95.5	
		3	1	100	92	
CuO SMSs @Cu foam	1 M LiTFSI in 1:1 (v/v) DOL/DME with 2% $LiNO_3$ (-)	1	1	500	98.6	4
Cu_xO NWs @Cu foam	1 M LiTFSI in 1:1 (v/v) DOL/DME with 1% $LiNO_3$ (60 μL)	1	1	350	99.5	5
		2	2	210	99.3	
		5	1	100	99	
Li_2O@Cu NWs@Cu foam	1 M LiTFSI in 1:1 (v/v) DOL/DME with 2% $LiNO_3$ (50 μL)	1	1	300	98.5	6
		1	2	150	96	
		2	2	100	93	
CuO NWs @Cu foam	1 M LiTFSI in 1:1 (v/v) DOL/DME with 1% $LiNO_3$ (80 μL)	0.5	1	280	96	7
		1	1	150	95.9	
		3	0.5	150	95	
CuON NAs	1 M LiTFSI in 1:1 (v/v)	0.5	1	450	97.9	8

@Cu foam	DOL/DME with 2% $LiNO_3$ (100 µL)	1	1	170	-	
		2	1	100	98	
Cu_2O NWs @Cu foam	1 M $LiPF_6$ in 1:1:1(v/v/v) EC/DMC/DEC (80 µL)	1	1	100	99	9
CoO NSs @Cu foam	1 M $LiPF_6$ in 1:1 (v/v) EC/DMC (-)	1	1	200	99.2	10
Au/Cu NNs @Cu foam	1 M LiTFSI in 1:1 (v/v) DOL/DME with 0.1% $LiNO_3$ (-)	1	1	100	96	11
1D@3D-Cu/Sb	1 M LiTFSI in 1:1 (v/v) DOL/DME with 1% $LiNO_3$ (80 µL)	1	1	140	96.8	**This Work**
		3	1	105	96.6	
		5	1	80	95.2	

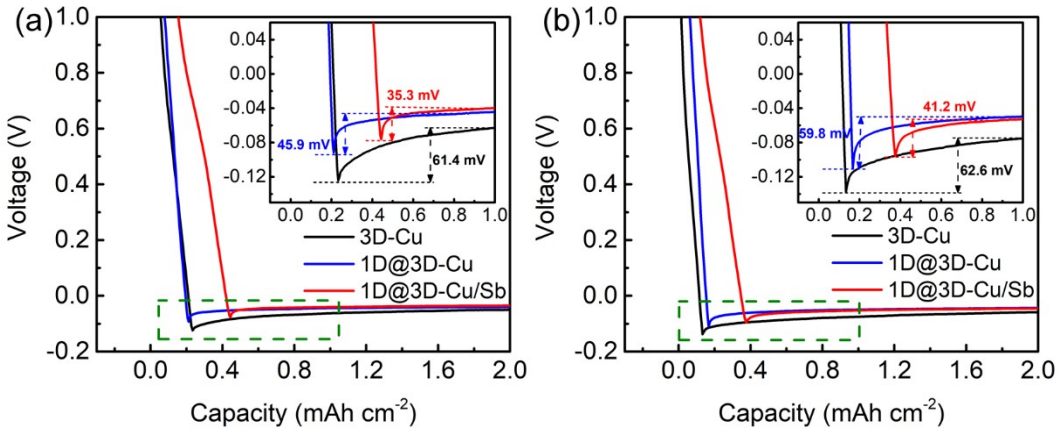

Figure S15. Nucleation overpotential of 3D-Cu, 1D@3D-Cu and 1D@3D-Cu/Sb at (a) 2 mA cm^{-2} (b) 3 mA cm^{-2}.

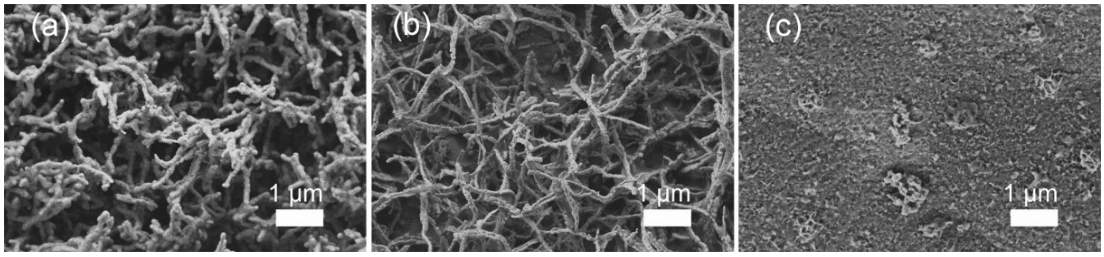

Figure S16. SEM images of (a) activated 1D@3D-Cu/Sb, (b) activated 1D@3D-Cu and (c) activated 3D-Cu.

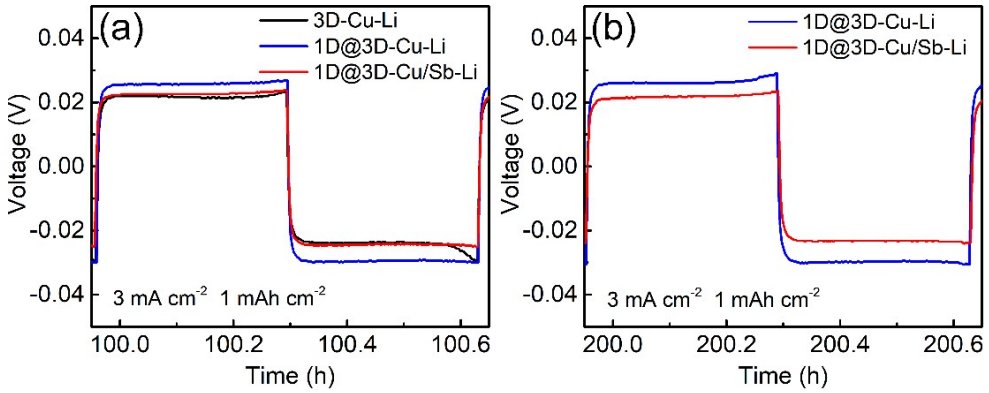

Figure S17. Voltage profiles of the Li||3D-Cu-Li, Li||1D@3D-Cu-Li and Li||1D@3D-Cu/Sb-Li symmetric cells at (a) 100 h and (b) 200 h.

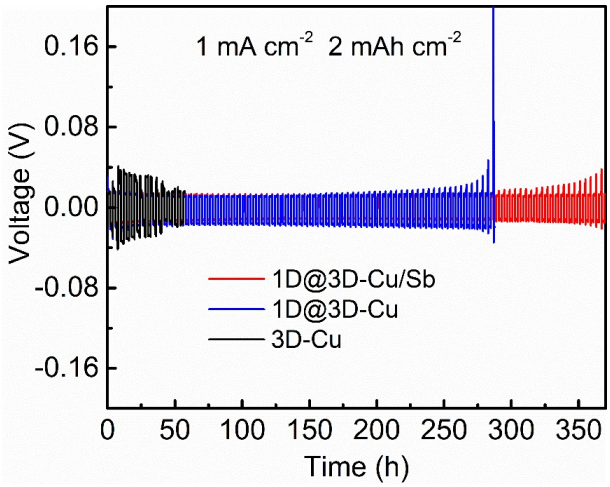

Figure S18. Voltage-time profiles of 3D-Cu-Li, 1D@3D-Cu-Li and 1D@3D-Cu/Sb-Li in symmetric cells at 1 mA cm^{-2} and 2 mAh cm^{-2}.

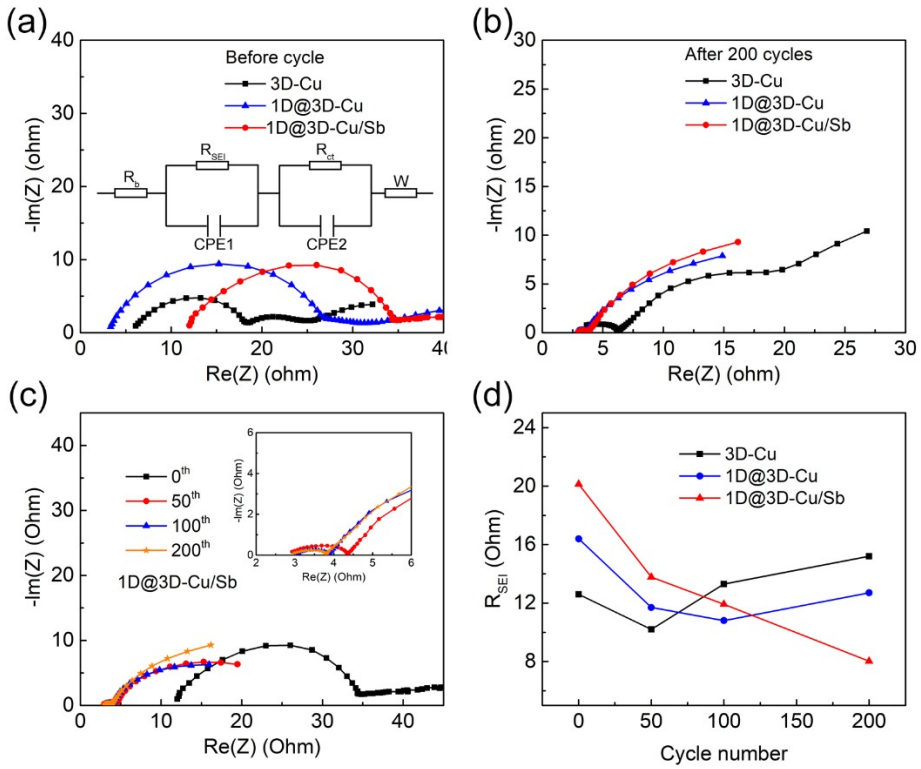

Figure S19. Nyquist plots and equivalent circuit of the symmetric cells (a) before cycling and (b) after 200 cycles at a current density of 3 mA cm^{-2}. (c) Nyquist plots of the symmetric cells with 1D@3D-Cu/Sb-Li electrode at different cycle numbers. (d) R_{SEI} vs. cycle number profiles of the symmetric cells with different electrodes.

Table S2. Electrochemical impedance fitted results of equivalent circuit models of the 3D-Cu-Li, 1D@3D-Cu-Li and 1D@3D-Cu/Sb-Li composite anode before and after 200 cycles.

	3D-Cu-Li		1D@3D-Cu-Li		1D@3D-Cu/Sb-Li	
	0 th	200 th	0 th	200 th	0 th	200 th
R_b [Ω]	6.5	2.77	2.95	2.81	12.4	2.98
R_{SEI} [Ω]	12.6	15.2	16.4	12.7	20.1	8.03
R_{ct} [Ω]	10.4	4.35	14.5	1.08	11.3	0.74

The SEI interfacial resistance (R_{SEI}) and the charge transfer impedance (R_{ct}) are associated with the semicircle at a high frequency range.[12, 13] The Nyquist plots and equivalent circuit were shown in Figure S19. The obtained values of the inter resistance (R_b), R_{SEI}, and R_{ct} were demonstrated in Table S2. R_{SEI} value of the 1D@3D-Cu/Sb electrode is 20.1 Ω for the pre-deposited cell and the value at the 200th cycle is 8.03 Ω, while these values for 1D@3D-Cu electrode are 16.4 and 12.7 Ω and these values for 3D-Cu electrode are 12.6 and 15.2 Ω, respectively. Meanwhile, the R_{ct} of symmetric cell based on 1D@3D-Cu/Sb electrode exhibits a much smaller value (0.74 Ω) in comparison with 1D@3D-Cu (1.08 Ω) and 3D-Cu (4.35 Ω) electrode after 200 cycles. As shown in Figure S7c, the impedance changes of Li||1D@3D-Cu/Sb-Li cell was reduced from the 50th cycle to the 200th cycle, implying the formation of a stable interface between 1D@3D-Cu/Sb-Li electrode and electrolyte.

Table S3. Comparison of the cycling performance of Li||Li symmetric cell between the 1D@3D-Cu/Sb current collectors and other lithiophilic Cu-based current collectors.

Current Collector	**Electrolyte & dosage**	**Current density [mA cm^{-2}]**	**Areal capacity [mAh cm^{-2}]**	**Time [h]**	**Voltage hysteresis [mV]**	**Ref.**
Cu fiber @Cu foam	1 M LiTFSI in 1:1 (v/v) DOL/DME with 0.4% $LiNO_3$ (-)	1	2	820	25	1
		3	1	280	30	
CuON NAs @Cu foam	1 M LiTFSI in 1:1 (v/v) DOL/DME with 2% $LiNO_3$ (100 μL)	2	1	2100	~5	8
		5	2	1600	~10	
Cu_xO NWs @Cu foam	1 M LiTFSI in 1:1 (v/v) DOL/DME with 1% $LiNO_3$ (60 μL)	1	1	1800	15	5
		2	2	1000	20	
CuO SMSs @Cu foam	1 M LiTFSI in 1:1 (v/v) DOL/DME with 2% $LiNO_3$ (-)	1	1	1150	-	4
		3	3	750	-	
Cu_2O NWs @Cu foam	1 M $LiPF_6$ in 1:1:1 (v/v/v) EC/DMC/DEC (80 μL)	1	1	1000	~10	9
		3	1	133	40	
CuO NWs @Cu foam	1 M LiTFSI in 1:1 (v/v) DOL/DME with 1% $LiNO_3$ (80 μL)	1	2	540	-	7
Li_2O@Cu NWs@Cu foam	1 M LiTFSI in 1:1 (v/v) DOL/DME with 2% $LiNO_3$ (50 μL)	1	1	600	15	6
		3	1	600	44	

LiF@Li-CuO@Cu foam	1 M $LiPF_6$ in 1:1 (v/v) EC/DEC (-)	1	1	600	5	14
		5	5	350	~198	
CoO NSs @Cu foam	1 M $LiPF_6$ in 1:1 (v/v) EC/DMC (-)	1	1	600	16	10
		8	1	150	50	
Cu_3N NRs @Cu foam	1 M $LiPF_6$ in 3:7 (v/v) EC/DEC with 5% FEC (-)	1	1	400	-	15
Au/Cu NNs @Cu foam	1 M LiTFSI in 1:1 (v/v) DOL/DME with 0.1% $LiNO_3$ (-)	1	0.5	970	-	11
1D@3D-Cu/Sb	1 M LiTFSI in 1:1 (v/v) DOL/DME with 1% $LiNO_3$ (80 µL)	1	1	900	~11	**This Work**
		1	2	370	~11	
		3	1	300	~20	

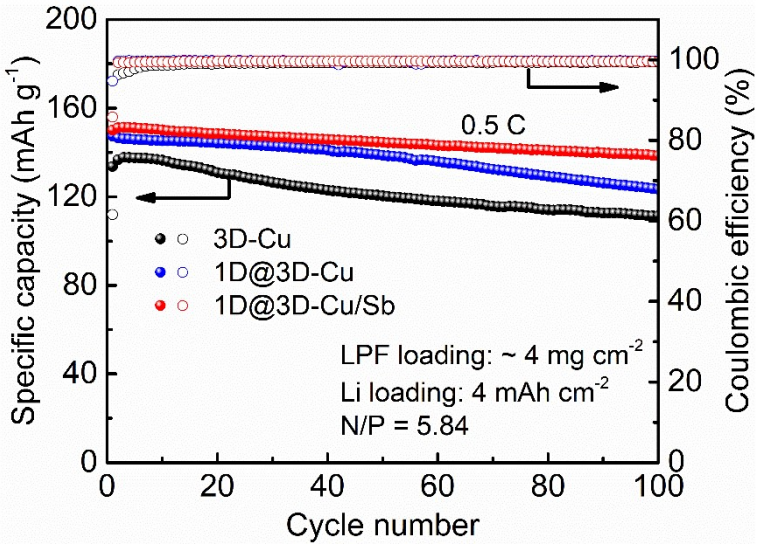

Figure S20. Cycling performance of full cells (N/P = 5.84) at 0.5 C (1 C = 170 mA g^{-1}).

Table S4. Comparison of the electrochemical performance of $LiFePO_4$||Li cell between the 1D@3D-Cu/Sb current collectors and other lithiophilic Cu-based current collectors.

Current collector	Electrolyte & dosage	Areal capacity of LFP	Areal capacity of Li	Rate [C]	Cycle number	Retention [%]	Ref.
Cu_2O NWs @Cu foam	1 M $LiPF_6$ in 1:1:1 (v/v/v) EC/DMC/DEC (80 μL)	5.5 mg cm^{-2}	-	1	100	-	9
Cu_2S NWs @Cu foam	1 M LiTFSI in 1:1 (v/v) DOL/DME with 1% $LiNO_3$ (40 μL)	6 mg cm^{-2}	2 mAh cm^{-2}	0.5	300	-	2
Cu_2S NWs @Cu foam	1 M LiTFSI in 1:1 (v/v) DOL/DME with 1% $LiNO_3$ (50 μL)	2.5 mg cm^{-2}	2 mAh cm^{-2}	0.5	100	96.5	3
CuON NAs @Cu foam	1 M LiTFSI in 1:1 (v/v) DOL/DME with 2% $LiNO_3$ (100 μL)	3.5 mg cm^{-2}	-	2	300	-	8
CuO NWs @Cu foam	1 M $LiPF_6$ in 1:1:1 (v/v/v) EC/DMC/EMC with 5% FEC (80 μL)	2 mg cm^{-2}	2 mAh cm^{-2}	2	150	-	7
Cu_xO NWs @Cu foam	1 M LiTFSI in 1:1 (v/v) DOL/DME	5 mg cm^{-2}	3 mAh	1	150	99.8	5

	with 1% $LiNO_3$ (60 µL)		cm^{-2}				
Li_2O@Cu NWs@Cu foam	1 M $LiPF_6$ in 1:1 (v/v) EC/DEC (-)	5 mg cm^{-2}	-	1	500	74.4	6
CoO NSs @Cu foam	1 M $LiPF_6$ in 1:1 (v/v) EC/DMC (-)	-	-	1	500	86.6	10
CuO SMSs @Cu foam	1 M LiTFSI in 1:1 (v/v) DOL/DME with 2% $LiNO_3$ (-)	1.2 mg cm^{-2}	5 mAh cm^{-2}	1	200	80	4
1D@3D-Cu/Sb	1 M LiTFSI in 1:1 (v/v) DOL/DME with 1% $LiNO_3$ (80 µL)	2 mg cm^{-2}	4 mAh cm^{-2}	0.5	200	81.4	**This work**
		4 mg cm^{-2}		0.5	100	92.4	

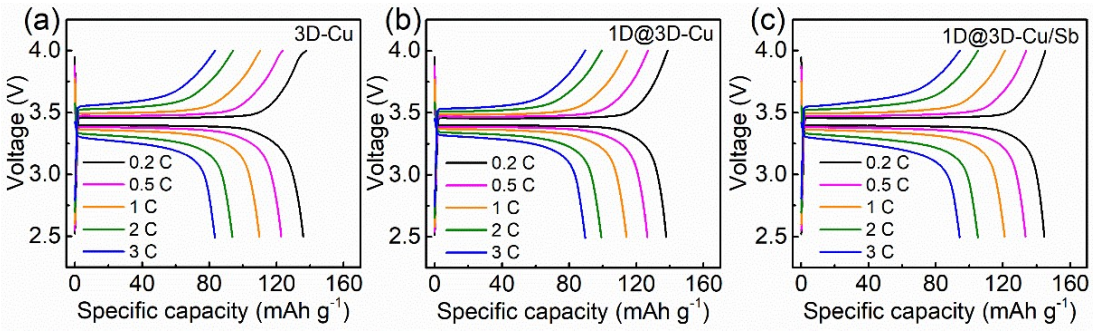

Figure S21. Charge/discharge curves of (a) 3D-Cu-Li||LFP, (b) 1D@3D-Cu-Li||LFP and (c) 1D@3D-Cu/Sb-Li||LFP full cells at various rates of 0.2, 0.5, 1, 2 and 3 C.

References

1. Y. Zhao, S. Hao, L. Su, Z. Ma and G. Shao, *Chem. Eng. J.*, 2020, **392**, 123691.

2. P. Zhai, Y. Wei, J. Xiao, W. Liu, J. Zuo, X. Gu, W. Yang, S. Cui, B. Li, S.

Yang and Y. Gong, *Adv. Energy Mater.*, 2020, **10**, 1903339.

3. Z. Huang, C. Zhang, W. Lv, G. Zhou, Y. Zhang, Y. Deng, H. Wu, F. Kang and Q.-H. Yang, *J. Mater. Chem. A*, 2019, **7**, 727-732.

4. Y. Jiang, B. Wang, A. Liu, R. Song, C. Bao, Y. Ning, F. Wang, T. Ruan, D. Wang and Y. Zhou, *Electrochim. Acta*, 2020, **339**, 135941.

5. R. Lu, B. Zhang, Y. Cheng, K. Amin, C. Yang, Q. Zhou, L. Mao and Z. Wei, *J. Mater. Chem. A*, 2021, **9**, 10393-10403.

6. L. Tan, X. Li, M. Cheng, T. Liu, Z. Wang, H. Guo, G. Yan, L. Li, Y. Liu and J. Wang, *J. Power Sources*, 2020, **463**, 228178.

7. J. Cao, L. Deng, X. Wang, W. Li, Y. Xie, J. Zhang and S. Cheng, *Energy Fuels*, 2020, **34**, 7684-7691.

8. M. Lei, Z. You, L. Ren, X. Liu and J.-G. Wang, *J. Power Sources*, 2020, **463**, 228191.

9. Y. Ma, Y. Gu, Y. Yao, H. Jin, X. Zhao, X. Yuan, Y. Lian, P. Qi, R. Shah, Y. Peng and Z. Deng, *J. Mater. Chem. A*, 2019, **7**, 20926-20935.

10. R. Zhang, Y. Li, M. Wang, D. Li, J. Zhou, L. Xie, T. Wang, W. Tian, Y. Zhai, H. Gong, M. Gao, K. Liang, P. Chen and B. Kong, *Small*, 2021, **17**, 2101301.

11. N. Luo, G. J. Ji, H. F. Wang, F. Li, Q. C. Liu and J. J. Xu, *ACS Nano*, 2020, **14**, 3281-3289.

12. X.-Y. Yue, W.-W. Wang, Q.-C. Wang, J.-K. Meng, Z.-Q. Zhang, X.-J. Wu, X.-Q. Yang and Y.-N. Zhou, *Energy Storage Mater.*, 2018, **14**, 335-344.

13. S.-S. Chi, Y. Liu, W.-L. Song, L.-Z. Fan and Q. Zhang, *Adv. Funct. Mater.*,

2017, **27**, 1700348.

14. Y. Feng, C. Zhang, B. Li, S. Xiong and J. Song, *J. Mater. Chem. A*, 2019, **7**, 6090-6098.

15. H. Park, J. Kwon, T. Song and U. Paik, *J. Power Sources*, 2020, **477**, 228776.